

Development of electromagnetic damper

Shanker Ganesh Krishnamoorthy*, Inga Skiedraitė**

*Kaunas University of Technology, Studentų St. 56, 51424 Kaunas, Lithuania, E-mail: shanker.krishnamoorthy@stud.ktu.lt

**Kaunas University of Technology, Studentų St. 56, 51424 Kaunas, Lithuania, E-mail: inga.skiedraite@ktu.lt

crossref <http://dx.doi.org/10.5755/j01.mech.21.3.9838>

1. Introduction

Mechanical vibration may be caused by force whose magnitude or direction or point of application varies with time. Vibration deals with force and motion, therefore it can be considered as subfield of dynamics. In some cases resulting vibrations may be of no consequences, in others they may be disastrous. Vibration may be undesirable because they can result in deflection of sufficient magnitude to lead to malfunction [1-3].

To reduce the impact of vibration force, damping is provided. The energy dissipation properties of material or a system under cyclic stress is known as damping [1-3]. Dampers are essential in reducing the vibration transmitted to a body. Dampers can be classified as passive and semi-active dampers [1-3]. Hydraulic damper comes under passive dampers [4]. Magnetorheological (MR) damper and electromagnetic dampers are classified under semi-active dampers [5-9].

The magnetic flux from electromagnet (EM) can be controlled by varying the current passing through electromagnet [10-12]. This type of electromagnet can be implemented in several fields of application in day to day life

[13-14]. Currently there exist many damping devices which work under the principal of electromagnetism. Various research and development are ongoing related to electromagnetic damping [10-18].

The idea of combination of three stages of damping, explained in this paper, was obtained from the principles of eddy current damping [11] (Fig. 1), the adaptive magnetic levitation system [19] (Fig. 2) and the working of shunt damping [20-28].

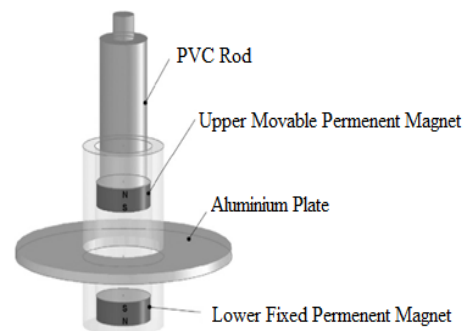


Fig. 1 The eddy current spring-damper [11]

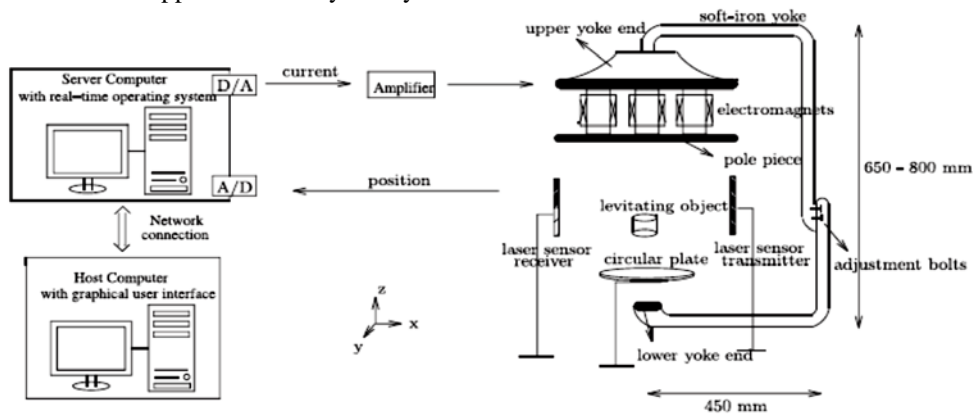


Fig. 2 Schematic of the magnetic levitation system [19]

From the investigation of existing dampers and taking into consideration, constructing a damper which is easy to construct, adaptive and cost-efficient, a device is proposed in this paper, where three stages of damping (Fig. 3) are combined to make an effective damping and to sustain a shock (vibration force) ranging from 10 to 50 N. The proposed technology can be used to replace the existing packing methods like bubble wraps, package cushioning for fragile items, thereby helps to provide a more reliable and real-time damping system. The wall of shock absorbing box can be constructed using the proposed EMD as shown in Fig. 4. The force transmitted from external wall of the box to the interior wall of the box will be reduced (damped) by the small units of EMD, which is

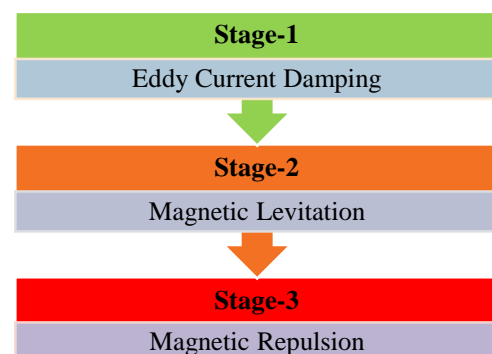


Fig. 3 Three stages of damping

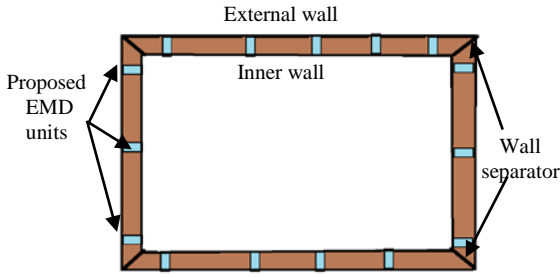


Fig. 4 Design of shock absorbing box

placed in between the walls. The idea and work for future development are innovative and can be applicable in transportation, medical and industrial fields.

Proposed working principle of electromagnetic damper (EMD) is shown in Fig. 5. Stage-1 damping is obtained due to the effect of eddy current formation, when the piston with the magnets moves through copper pipe (Fig. 5). Stage-2 damping is obtained when the magnet enters the region of solenoid setup and starts to levitate and there by resist the downward movement of magnet (Fig. 5). When the force acting on the piston is larger, then magnetic levitation breaks and piston moves downward. To resist the downward movement of the piston stage-3 damping is provided, in which the electromagnet is used to repel the permanent magnet upward (Fig. 5)

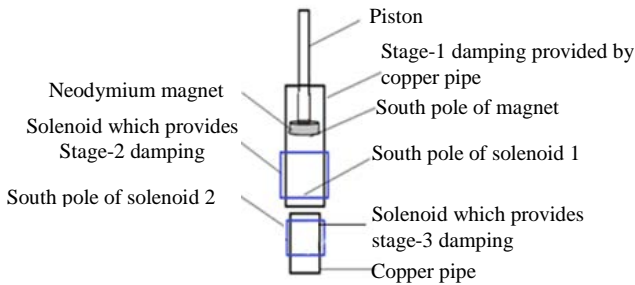


Fig. 5 Proposed working principle of EMD

2. Mathematical modelling of damper system

For better understanding of the prototype and based on required design parameters and to find out the excitation of force from base to top platform, a mathematical modelling was done for a damper system with single degree of freedom.

If the spring supplies a restoring force proportional to its elongation and the dashpot (electromagnetic damper) provides a force which opposes motion of the mass proportional to its velocity, then the system response is proportional to the excitation, and the system is said to be linear [29, 30]. Therefore the mathematical model developed will be linear single degree of freedom system.

Base motion of a damper system with a single degree of freedom is shown in the Fig. 6, in which K is the spring constant of spring and c is the damping coefficient.

The modelling of spring was done as per the prototype and some assumptions were made. These are summarised in Table 1. The shaded sections are the values assumed and the other values were determined as per the calculation using respective formulas [29, 30].

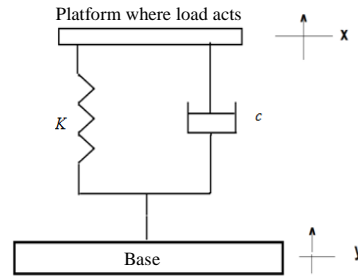


Fig. 6 A damper system with a single degree of freedom

Table 1

Summary of values for modelling of EMD

Spring constant K	1.52 N/mm
Mass of platform M	1 kg
Maximum load	24.32 N
Natural frequency ω_n	0.39 Hz
Forcing frequency f	1 Hz
Forcing ratio r	2.56
Damping ratio ζ	0.5
Damping coefficient c	3.86 Ns/m

The above results are applied in proposed model of single degree of freedom system. The system is shown in Fig. 7.

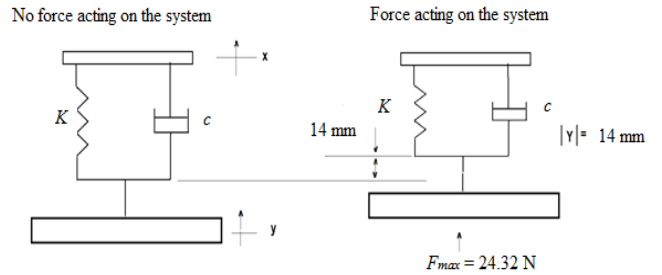


Fig. 7 Scheme of force acting on the EMD

Consider $y(t)$ represents the motion of the base center, the base is subjected to external forces as shown in Fig. 7. The vertical motion X of top platform, is determined from [30]:

$$\left| \frac{X}{Y} \right| = \left(\frac{(1 + (4\zeta^2 - 1)r^2)^2 + (2\zeta r^3)^2}{(1 - r^2)^2 + (2\zeta r)^2} \right)^{\frac{1}{2}}$$

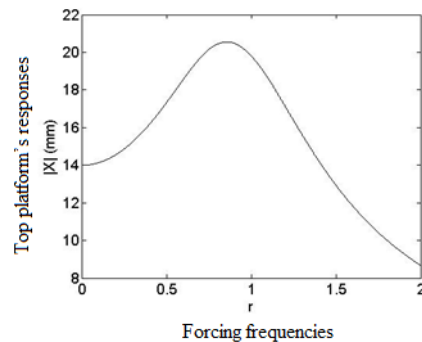


Fig. 8 Top platform's responses X to forcing frequencies r

The 14 mm excitation of base is transmitted as magnitude of oscillation, $|X| = 7.544$ mm to the top platform of mass M (1 kg). This amplification occurs because the assumption forcing frequency (1 Hz) is near the suspension's natural frequency (0.39 Hz).

A graph between top platform's responses, X , to forcing frequencies r , obtained using *MATLAB* (Fig. 8).

3. Investigation on three stages of damping and results

Stage-1 damping. Stage-1 damping is obtained by Eddy current damping. Eddy currents are generated in a conductor in a time-varying magnetic field [31]. They are induced either by the movement of the conductor in the static field or by changing the strength of the magnetic field, initiating motional and transformer electromotive forces, respectively. Since the generated eddy currents create a repulsive force that is proportional to the velocity of the conductor, the moving magnet and conductor behave like a viscous damper. The diagrammatic representation of the magnet falling through the metal pipe is shown in Fig. 9.

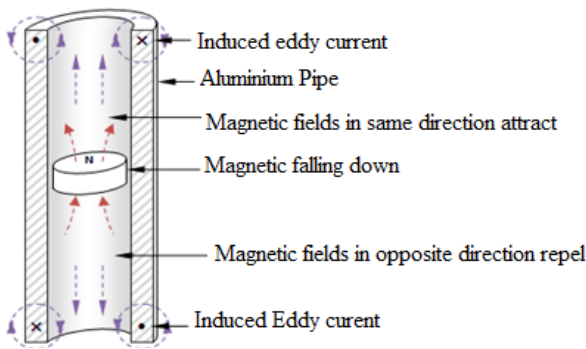


Fig. 9 Diagrammatic representation of the magnet falling through the metal pipe [31]

The stage-1 is investigated by the free fall of Neodymium magnet of 20 mm diameter and 0.2 mm thick through copper pipe 160 mm long and 28 mm diameter. The results of observations are given in Table 2.

From Table 2 it is clear that when the magnetic field of magnet is increased, then the time taken by the magnet to cover 160 mm length copper pipe in freefall also increases. This states that, when magnetic field of permanent magnet increases, the Eddy current induced in the copper pipe also increases there by providing a damping effect.

Table 2

Stage-1 results

Number of magnets attached, units	Time taken to cover 160 mm in free fall, ms
1	23
2	35
3	50
4	55
5	85
6	98

Modelling of stage-1 damping. To justify the above experiment, modelling of free fall of magnet through copper pipe was done using *COMSOL Multiphysics*. Simulation of the magnetic flux density formed inside the copper pipe at time $t = 50$ ms from the start of free fall of magnet inside the copper pipe is shown in Fig. 10.

Simulation of the current density (Eddy current) formed when the magnet moves and reaches the centre of the copper pipe (time $t = 50$ ms) is shown in Fig. 11.

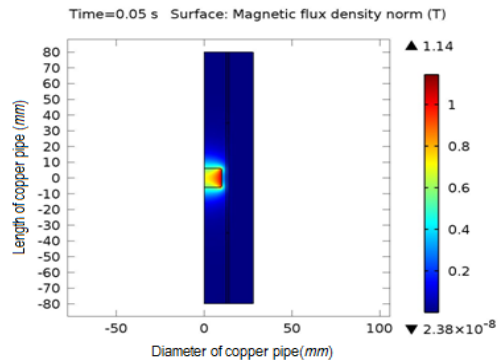


Fig. 10 Simulation of the magnetic flux density, when magnets reach at centre of copper pipe

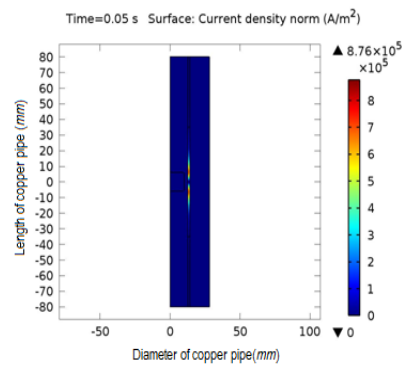


Fig. 11 Simulation of the current density (Eddy current) formed when the magnet moves and reaches the centre of the copper pipe

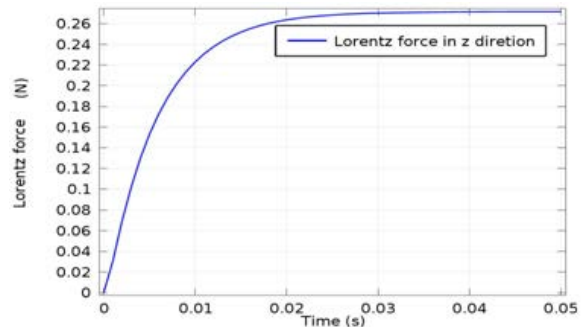


Fig. 12 Observation of Lorentz force acting on the free fall of magnet

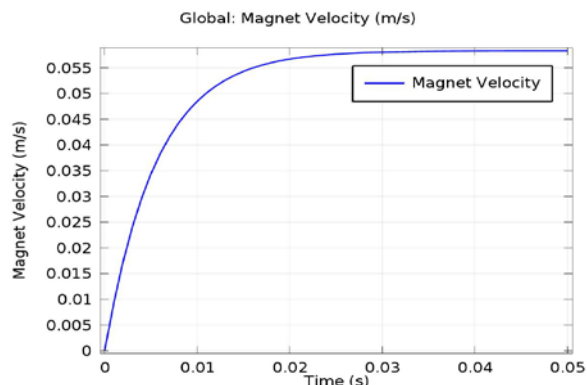


Fig. 13 Observation of velocity of free fall of magnet through copper pipe

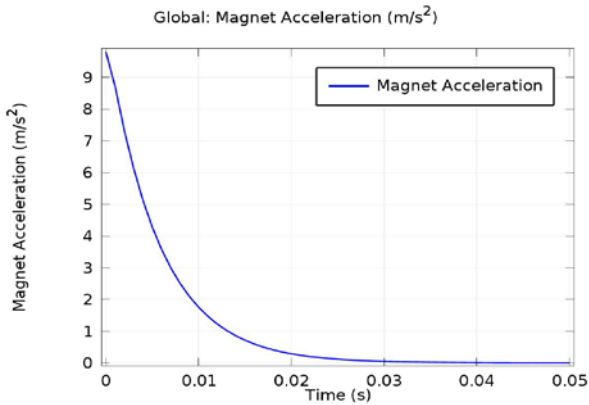


Fig. 14 Observation of acceleration of free fall of magnet through copper pipe

The effect of Eddy current damping can be explained using the gradual increases, in case of Lorentz force and velocity and after a time 50 ms both become constant, in the case of magnet falling freely inside a copper pipe. Whereas the acceleration reduces and become constant. The respective cases can be justified using the graph obtained from the modelling of stage-1 experiment (Figs. 12, 13 and 14).

Stage-2 damping. For stage-2 damping, different types of solenoids were constructed and tested, in order to understand the nature of magnetic field formed inside the solenoid. Each types differ from each other by number of windings, number of layer of windings, combination of magnetic poles on coil, by varying the current through coil and making of split coils. Among this a simple solenoid construction with number of windings N (90), with 2 layers and length of solenoid L (50 mm) was chosen.

The main objective of stage-2 investigation is to study the nature of behaviour of magnetic field inside the solenoid by determining the magnetic field theoretically as well as from modelling and observe the nature of a permanent magnet levitating inside the solenoid.

Solenoid is a long straight coil of wire that can be used to generate a nearly uniform magnetic field similar to that of a bar magnet (Fig. 15) [32]. The field can be greatly strengthened by the addition of an iron core.

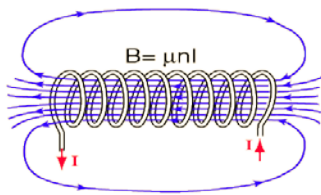


Fig. 15 Distribution of magnetic field along solenoid [32]

At the centre of a long solenoid, the magnetic field is [32]:

$$B = \mu nI. \tag{1}$$

From Eq. (1) for the magnetic field B , n is the number of turns per unit length (turn's density), I – current passing through the wire, μ is the permeability ($\mu = k\mu_0$ and $\mu_0 = 4\pi \times 10^{-7} \text{ H m}^{-1}$), k is relative permeability of core. The core used here is a copper pipe. Permeability of copper pipe is 0.999994 (permeability of air is 1.00000037 [33]).

Hence value of k is taken to be 1 for theoretical experiment and also for finite element modelling. The turn density is denoted as $n = N/L$, where N is number of turns and L is length of solenoid.

A simple solenoid was constructed with copper pipe of 0.2 mm thick as the core and the number of turns (winding of insulated copper wire) N (90) and length of solenoid L (50 mm) was made (Fig. 16).

Experimental setup is shown in Fig. 16. The value of magnetic field at the centre of the solenoid is determined theoretically using Eq. (1). Theoretically the expected magnetic field B is calculated as $2.261946711 \times 10^{-3} \text{ T}$.

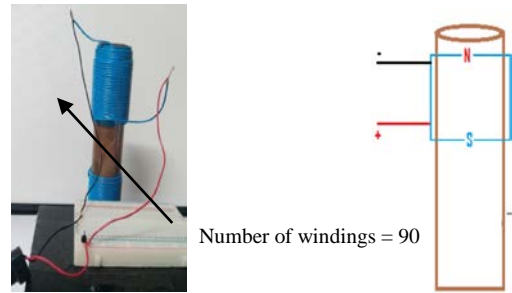


Fig. 16 Experimental setup for stage-2

Modelling of stage-2 damping. The modelling of above experimental setup is done using the software *Vizimag*. Magnetic field line representation and magnetic flux density of at the centre of solenoid is shown in figure Fig. 17. The maximum flux density B_{max} , force around solenoid P due to magnetic field and magnetic field density at the centre of the core B obtained from modelling of stage-2 setup is shown in Table 3.

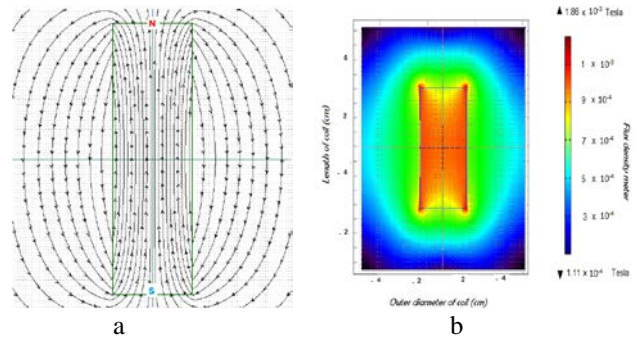


Fig. 17 Modelling of stage-2: a - magnetic field line representation, b - magnetic flux density

Table 3

Results from modelling

B_{max}	$1.89 \times 10^{-3} \text{ T}$
P (force around solenoid)	$5.55 \times 10^{-6} \text{ N}$
B (magnetic flux density at centre of solenoid)	$1.528 \times 10^{-3} \text{ T}$

To know the nature of levitation inside solenoid a piece of neodymium magnet was allowed to fall freely through solenoid setup. It was observed that the neodymium magnet was able to levitate inside the solenoid; this is shown in Fig. 18, a and schematic drawing of magnet aligning inside the solenoid is shown in Fig. 18, b.

For an extra external force while magnet falls freely, a 12 g of weight (e.g.: bolt) which is equivalent 1.18 N on free fall is attached to the magnet. For an extra external force during the free fall of magnet a weight is

attached with single disc magnet is shown in Fig. 19, a and with multiple magnets is shown in Fig. 19, b.

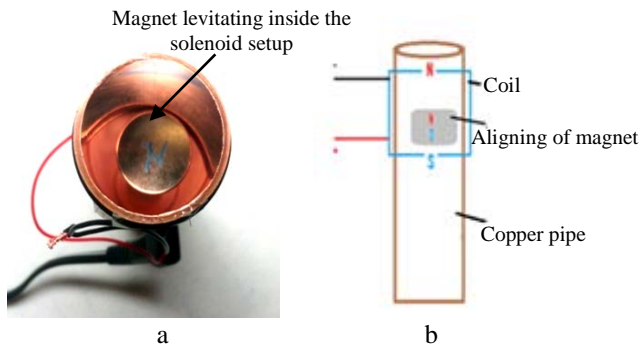


Fig. 18 Levitation of one piece of magnet inside solenoid: a - from experimental setup; b - schematic drawing

It was observed that the magnet with extra weight was able to levitate. As the magnets increased the strength of levitation also increased. On varying external force acting on the levitating unit (the magnet with attached weight), was able to reciprocate.

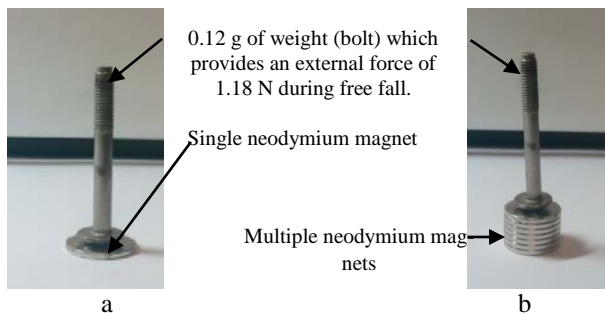


Fig. 19 For an extra external force during the free fall of magnet: a - weight attached with single unit of magnet, b - weight attached with multiple units of magnets

Stage-3 damping is provided by magnetic repulsion between the edges of solenoid and magnet. Simple solenoid construction with copper pipe of 0.2 mm thick and outer diameter 18 mm is used as inner core of solenoid 2. The number of turns N (90) and length of solenoid is L (50 mm). The solenoid setup is as shown in Fig. 20.

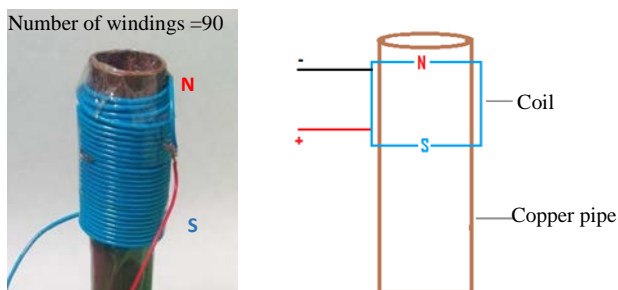


Fig. 20 Experimental setup of stage-3

There is a magnetic field produced inside the solenoid which is theoretically determined from Eq. (1). Theoretically the expected magnetic field B is calculated as $2.261946711 \times 10^{-3}$ T.

Modelling of stage-3 damping. The magnetic field line representation and magnetic flux density of stage-3

damping system is shown in Fig. 21. The maximum flux density B_{max} , Force around solenoid P due to magnetic field and magnetic field density at the centre of the core B obtained from modelling of stage-3 setup is shown in Table 4.

Table 4

Results from stage-3 modelling

B_{max}	3.63×10^{-3} T
P (force around solenoid)	1.57×10^{-5} N
B (magnetic flux density at centre of solenoid)	3.687×10^{-3} T

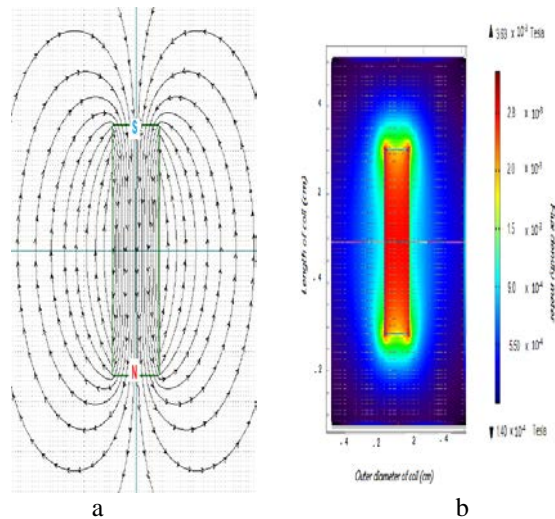


Fig. 21 Modelling of stage-3: a - magnetic field line representation, b - magnetic flux density

Fig. 22 illustrate the experimental setup of stage-3 damping. Fig. 22, a shows that the magnet repels when south pole of magnet comes in contact with south pole of solenoid. Fig. 22, b shows that when north pole of magnet come in contact with south pole of solenoid both unit get attracted and rests over the solenoid. For stage-3 damping we will be using experimental setup as shown in Fig. 22, a.

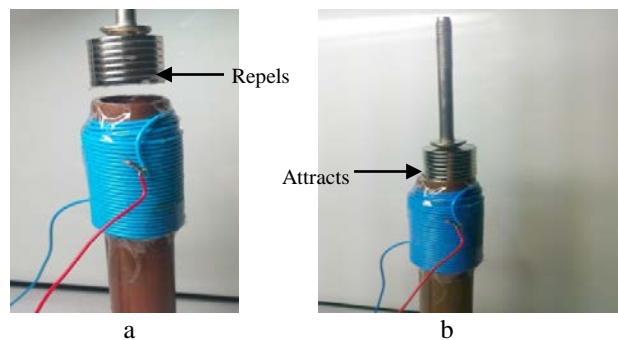


Fig. 22 Experimental view of stage-3 damping: a - magnet repelled when south poles comes in contact, b - magnet attracts when north pole comes in contact

4. Design and prototyping of EMD

4.1. Design of proposed EMD

The design of the proposed EMD is shown in Fig. 23. The EMD is placed between load acting platform and a base. The main part of the construction consists of

the spring, neodymium magnet and solenoid setup. The other parts are: piston (which connects the load acting platform and the magnet arrangement), spring holder and a coupling (which helps to couple the solenoid 1 and the outer cover of the solenoid 2).

Parts are shown in Fig. 23. It consists of two solenoids: solenoid 1 made from copper pipe of 28 mm diameter and 100 mm length and solenoid 2 made from copper pipe of 18 mm diameter and 50 mm length. A spring of outer diameter 27 mm, 7 units of permanent magnet, 90 mm long piston which holds the permanent magnet, outer cover of solenoid 2, coupling for coupling two solenoid section and a spring holder.

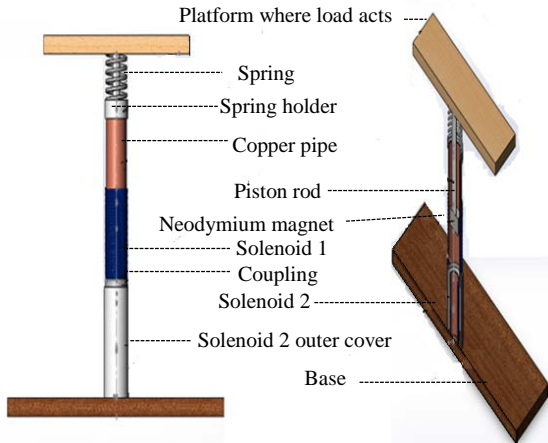


Fig. 23 Proposed EMD

4.2. Control system of proposed EMD

The control system for EMD is shown in Fig. 24. The purpose of the control system is to sense the distance between two walls (platform where the load acts and the base), and there by activate the solenoids to resist the frequent and sudden downward movement of permanent magnets. When the distance between the walls varies, it is detected by the proximity sensor. The output from proximity sensor is send to microcontroller in the form of analogue signals. Micro controller is programmed in such a way that it produces output signal to the driver module board to activate solenoid 1 and solenoid 2 respectively (Fig. 24).

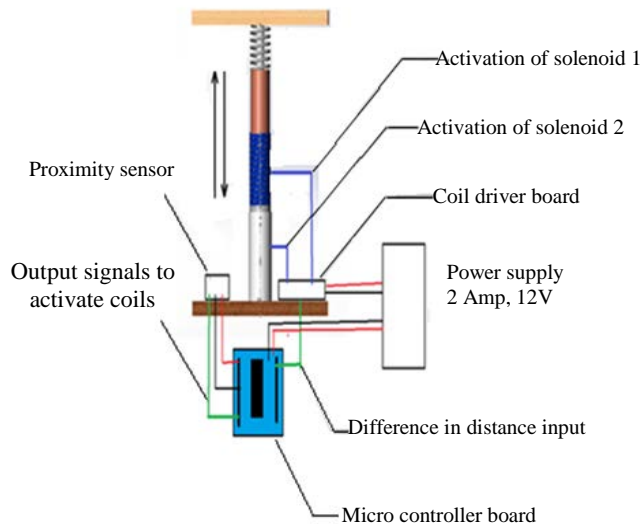


Fig. 24 The control system for EMD

The microcontroller will be programmed to emit digital signal to the controller according to the distance diagram in Fig. 25. The signal will be adjusted using feedback signals from the proximity sensors. Driver act as a digital-to-analogue signal convertor. The process continues as long as there will be force acting on the system. Initially the distance between the platform where load act and sensor is read and when the sensor reads distance between the regions *a* solenoid 1 is activated and when sensor reading is between *b* solenoid 2 is activated. The parameters *a* and *b* depends on the placing of sensor module.

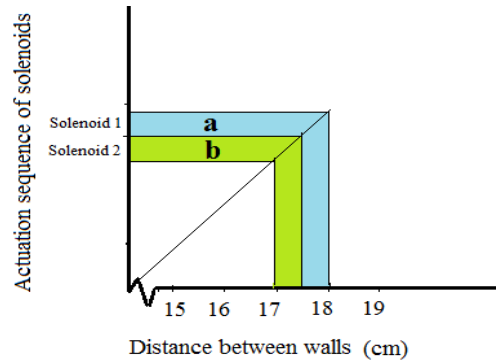


Fig. 25 Actuation sequence of solenoid

The control system is supported by a feedback system as shown in Figs. 26 and 27. Considering a simple system characterized by a single variable *L* which represents the distance between base and load acting platform. Under normal conditions the system has a steady state value of $L=L_0$ which may vary somewhat over time due to the variation of force acting *f*, on the load acting platform which cannot be measured or are unaware. To rectify the variation in the value of *L* as a result of varying force a mechanism for measuring the state of the system as well as a control input *i*, with which can be used to modify the state *L* of the system. In summary, the system has the following functional form $L(i; f; t)$. Fig. 26 shows a block diagram of the relationship between the system, the variables *i* and *f*, and the measurement of the system state *L*. Created according to feedback and PID control theory [34].

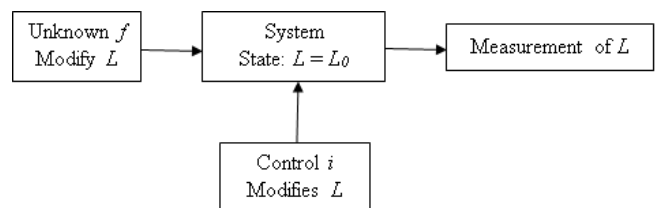


Fig. 26 Block diagram of the relationship between the system's *L*, *f* and *i*

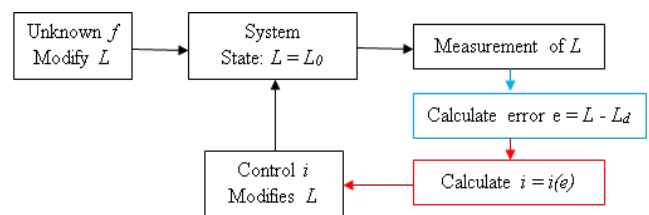


Fig. 27 Block diagram of system with the feedback loop

Fig. 27 illustrates the block diagram of system with the feedback loop. In which an unknown force *f* modi-

fies the distance between two wall L and a new value for the distance between the walls L_d . An error e is calculated by taking the difference between L and L_d . The input which is a function of error e , calculates the error and send it to the controller to modify L .

Final assembly (Fig. 28) shows the complete set-up of proposed EMD. This consists of the EMD device (assembled EMD), micro controller module with driver module, digital sensor module, external power supply and LED lights.

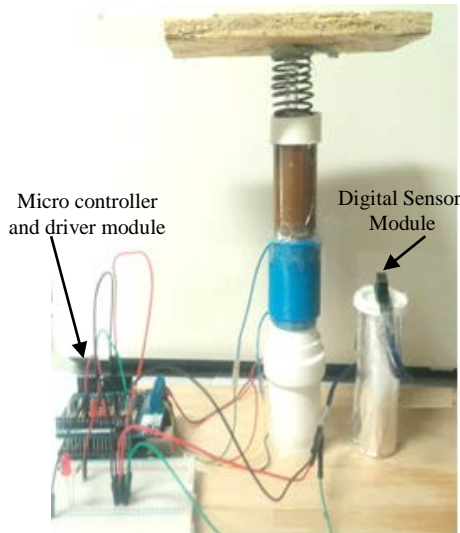


Fig. 28 Final assembly of EMD

5. Conclusions

In this paper an adaptive and semi active EMD is developed, by implementing proposed idea of combination of three stages of damping. The proposed EMD can be used to damp forces between 10-50 N and one of its major application is in developing a shock absorbing box, which can be used for the transportation of fragile and valuable materials.

Mathematical modelling of damper system (single-degree-of-freedom system) for the proposed system was modelled. It was observed that an excitation of 14 mm on the base of system is transmitted as 7.554 mm on top platform. Based on this modelling, a damper was constructed by implementing the three stages of damping which includes the technology of electromagnets and permanent magnet.

References

1. **Russell Richards.** 2007. Comparison of Linear, Non-linear, Hysteretic, and Probabilistic MR Damper Models. Master project, Virginia Polytechnic Institute and State University. 99p, [online] [accessed 15 February 2014]. Internet source: http://scholar.lib.vt.edu/theses/available/etd-03112007-24350/unrestricted/RJ_Richards_Thesis.pdf.
2. **Ragelio Palomera Arias.** 2005. Passive Electromagnetic Damping device for motion control of building structures. Doctor of Philosophy in Architecture: Building Technology. Massachusetts Institute of Technology. 146p. <http://dx.doi.org/http://hdl.handle.net/1721.1/33174>.
3. **David, I. G. Jones.** 2001. Handbook of Visco-elastic Vibration Damping.- John Wiley & Sons Ltd. 389p.
4. **Masi, J.W.** 2001. Affective of Control Techniques on the Performance of Semiactive Dampers. Master of Science Project: Department of Mechanical Engineering, Virginia Tech. 184p. <http://hdl.handle.net/10919/30851>.
5. Lord Corporation .Rheonetic™ MR Damper RD-1005-3 [online] [accessed 15 August 2014]. Internet source: http://www.rheonetic.com/devices_damper_begin.htm
6. **Simon, D.** 2001. Investigation of the Effectiveness of Skyhook Suspension for Controlling Roll Dynamics of Sport Utility Vehicles using Magneto-Rheological Dampers, Ph.D. Dissertation: Department of Mechanical Engineering, Virginia Tech. 202p. <http://scholar.lib.vt.edu/theses/available/etd-12032001-202230>.
7. **Ma, X.Q.; Wang, E.R.; Rakheja, S.; Su, C.Y.** 2002. Modeling hysteretic characteristics of MR fluid damper and model validation. Proceedings of the 41st IEEE Conference on Decision and Control. Las Vegas, NV. <http://dx.doi.org/10.1109/CDC.2002.1184761>.
8. **Spencer, B.F.; Dyke, S.J.; Sain, M.K.; Carlson, J.D.** Phenomenological model for a magnetorheological damper, J. Eng. Mech. Am. Soc. Civil Eng. 123: 230-252. [http://dx.doi.org/10.1061/\(ASCE\)0733-9399\(1997\)123:3\(230\)](http://dx.doi.org/10.1061/(ASCE)0733-9399(1997)123:3(230)).
9. **Dominguez, A.; Sedaghati, R.; Stiharu. I.** 2004. Modeling the hysteresis phenomenon of megnetorheological dampers, Smart Materials and Structures 13: 1351-1361p. <http://dx.doi.org/10.1088/0964-1726/13/6/008>.
10. **Wen-ai, Shen; Songye, Zhu; You-lin, Xu.** 2012. An experimental study on self-powered vibration control and monitoring system using electromagnetic TMD and wireless sensors, Sensors and Actuators A 180: 166-176. <http://dx.doi.org/doi:10.1016/j.sna.2012.04.011>.
11. **Ebrahimia, Babak; Khamesee, Mir Behrad; Golnaraghi, M. Farid.** 2008 Design and modeling of a magnetic shock absorber based on eddy current damping effect, Journal of Sound and Vibration 315(4-5): 875-889. <http://dx.doi.org/10.1016/j.jsv.2008.02.022>.
12. **Alanoly, J.; Sankar, S.** 1986. A new concept in semi-active vibration isolation, ASME Design Engineering Technical Conference 86-DET-28: 291-309. <http://dx.doi.org/10.1115/1.3267444>.
13. **Arsem, H.B.** 1971. Electric shock absorber, US. Patent Number 3559027 .
14. **Aspinall, D.T.; Oliver, R.J.** 1964. Vehicle riding comfort: the correlation between subjective assessments of vehicle ride and physical measurements of vehicle motion, Publisher: Motor Industry Research Association report.
15. **Bae, J.S.; Kwak, M.K.; Inman, D.J.** 2005 Vibration suppression of cantilever beam using eddy current damper, Journal of Sound and Vibration 284(3-5): 805-824. <http://dx.doi.org/10.1155/2014/893914>.
16. **Barak, P.** 1992. Passive versus active and semi-active suspension from theory to application in north American industry, SAE Technical Paper 922140.

- <http://dx.doi.org/10.4271/922140>.
17. **Bernard, J.; Shannan, J.; Vanderploeg, M.** 1991. Vehicle rollover on smooth surface, SAE Technical Paper Series, 891991.
<http://dx.doi.org/10.4271/891991>.
 18. **Graves, K.E.; Toncich, D.; Iovenitti, P.G.** 2000. Theoretical comparison of motional and transformer EMF device damping efficiency, *Journal of Sound and Vibration* 233: 441-453.
<http://dx.doi.org/10.1006/jsvi.1999.2820>.
 19. **Elliott, Stephen J.; Zilletti, Michele.** 2014. Scaling of electromagnetic transducers for shunt damping and energy harvesting, *Journal of Sound and Vibration* 33: 2185-2195.
<http://dx.doi.org/10.1016/j.jsv.2013.11.036>.
 20. **Fleming, Andrew J.; Moheimani, S.O. Reza.** 2006. Inertial vibration control using a shunted electromagnetic transducer, *IEEE/ASME Transactions on Mechatronics* 11: 84-92.
<http://dx.doi.org/10.1109/TMECH.2005.863364>.
 21. **Paulitsch, C.; Gardonio, P.; Elliott, S.J.** 2007. Active vibration damping using an inertial, electro-dynamic actuator, *ASME Journal of Vibration and Acoustics* 129(1): 39-47.
<http://dx.doi.org/10.1115/1.2349537>.
 22. **Glynne-Jones, P.; Tudor, M.J.; Beeby, S.P.; White, N.M.** 2004. An electromagnetic, vibration-powered generator for intelligent sensor systems, *Sensors and Actuators A: Physical* 110(1-3): 344-349.
<http://dx.doi.org/10.1016/j.sna.2003.09.045>.
 23. **Nakano, K.; Elliott, S.J.; Rustighi, E.** 2007. A unified approach to optimal conditions of power harvesting using electromagnetic and piezoelectric transducers, *Smart Materials and Structures* 16(4): 948-958.
<http://dx.doi.org/10.1088/0964-1726/16/4/002>.
 24. **Hagood, N.W.; von Flotow, A.** 1991. Damping of structural vibrations with piezoelectric material and passive electrical networks, *Journal of Sound and Vibration* 146: 243-268.
[http://dx.doi.org/10.1016/0022-460X\(91\)90762-9](http://dx.doi.org/10.1016/0022-460X(91)90762-9).
 25. **Moheimani, S.O.R.** 2003. A survey of recent innovations in vibration damping and control using shunted piezoelectric transducers, *IEEE Transactions on Control Systems Technology* 11: 482-494.
<http://dx.doi.org/10.1109/TCST.2003.813371>.
 26. **Cheng, T.H.; Xuan, D.J.; Li, Z.Z.; Shen, Y.D.** 2010. Vibration control using shunted electromagnetic transducer, *Applied Mechanics and Materials* 26-28: 905-908.
<http://dx.doi.org/10.4028/www.scientific.net/AMM.26-28.905>.
 27. **Rothemann, L.; Schretter, H.** 2010. Active vibration damping of the alpine ski, *Procedia Engineering* 2(2): 2895-2900.
<http://dx.doi.org/10.1016/j.proeng.2010.04.084>.
 28. **Scruggs, J.T.; Iwan, W.D.** 2005. Structural control with regenerative force actuation networks, *Structural Control and Health Monitoring* 12(1): 25-45.
<http://dx.doi.org/10.1002/stc.50>.
 29. **Rothbart, Harold A.; Hauserman, R.W.; Smith, S.M.; Schmidt, D.F.** 1996 *Mechanical Design Handbook* :-McGraw-Hill Press. 1400p.
 30. **Schmitz, T.L.; Smith, K.S.** 2012. *Mechanical Vibration - Modelling and measurements*. Springer Publishers. 373p.
 31. The relative motion between a conductor and magnetic field is used to generate an electrical voltage, [online] [accessed 9 June 2014]. Internet source: http://www.boredofstudies.org/wiki/The_relative_motion_between_a_conductor_and_magnetic_field_is_used_to_generate_an_electrical_voltage.
 32. Solenoid. [online] [accessed 20 July 2014]; Internet source: <http://hyperphysics.phy-astr.gsu.edu/hbase/hph.html>.
 33. Permeability, Wikipedia, [online] [accessed 20 July 2014]. Internet source: [http://en.wikipedia.org/wiki/Permeability_\(electromagnetism\)](http://en.wikipedia.org/wiki/Permeability_(electromagnetism)).
 34. Feed Back And PID Control Theory -1,[online] [accessed 15 August 2014]. Internet source: <http://www.wm.edu/about/search/index.php?q=pid+feedback>.

Shanker Ganesh Krishnamoorthy, Inga Skiedraitė

DEVELOPMENT OF ELECTROMAGNETIC DAMPER

S u m m a r y

This paper presents the development of an electromagnetic damper on proposed system of three stages of damping. Mechanical design, control system and control algorithm was developed for EMD. Control algorithm for EMD was explained by considering feedback system, and choosing control elements, sensor. Investigation was done regarding the three stages of damping. Based on the experimental setup theoretical evaluations as well as finite element modelling was done. The possible application of proposed EMD is mentioned in this paper.

Keywords: electromagnetic damper (EMD), eddy current damping, magnetic levitation, magnetic repulsion, solenoid.

Received February 12, 2015

Accepted May 06, 2015